Wnt gene regulation and function during maxillary palp development in *Drosophila melanogaster*

Michaela Holzem[1,2,*], Franziska A. Franke[1], Cláudia C. Mendes[1,3] and Alistair P. McGregor[1,*]

[1] Department of Biological and Medical Sciences, Faculty of Health and Life Sciences, Oxford Brookes University, Oxford, OX3 0BP, United Kingdom.

[2] Division of Signalling and Functional Genomics, German Cancer Research Centre (DKFZ), Heidelberg, Germany and Department of Cell and Molecular Biology, Medical Faculty Mannheim, Heidelberg University, Heidelberg, Germany.

[3] Department of Physiology, Anatomy and Genetics, University of Oxford, Oxford, OX1 3QX, United Kingdom.

* Corresponding authors: m.holzem@dkfz-heidelberg.de and amcgregor@brookes.ac.uk

Abstract

Wnt genes encode secreted ligands that play many important roles in the development of metazoans. There are thirteen known Wnt gene subfamilies and seven of these are represented in *Drosophila melanogaster.* While *wingless* (*wg*) is the best understood and most widely studied Wnt gene in *Drosophila*, the functions of many of the other *Drosophila* Wnt genes are less well understood. For example, relatively little is known about *Wnt6*, which is an ancient paralog of *wg* and they form a conserved Wnt cluster together with *Wnt9 (Dwnt4)* and *Wnt10*. *wg* and *Wnt6* encode similar proteins and exhibit overlapping expression in several tissues during development. Both *wg* and *Wnt6* were previously shown to regulate the development of maxillary palps, important olfactory organs in flies, but it remained unclear how these two ligands may combine to carry our specific functions and how this is regulated. Here, we have further analysed *Wnt6* function in the context of maxillary palp development. Surprisingly, we found that *Wnt6* does not appear to be necessary for development of maxillary palps. While a deletion of the 5' region of *Wnt6* results in very small maxillary palps, we show that this effect is more likely to be a consequence of removing *cis*-regulatory elements that may regulate *wg* expression in this tissue rather than through the loss of *Wnt6* function. Although, we cannot completely exclude the possibility that *Wnt6* may subtly regulate maxillary palp development in combination with *wg*, our analysis of *Wnt6* loss of function mutants suggests this ligand plays a more general role in regulating growth during development. Taken together our results provide new insights into maxillary palp formation and *Wnt6* functions in *Drosophila*, and further evidence for a complex cis-regulatory landscape in the *Wnt9-wg-Wnt6-Wnt10* cluster, which may help explain its evolutionary conservation.

Introduction

Wnt genes regulate a wide range of processes in metazoan cell biology, development and physiology (Logan and Nusse, 2004; Wiese et al., 2018). It has been shown that there are thirteen Wnt gene subfamilies and this diverse repertoire evolved early in metazoan evolution, although there has been subsequent loss and/or duplication of some of these genes in many lineages (Cho et al., 2010; Janssen et al., 2010; Lengfeld et al., 2009; Prud'homme et al., 2002).

Many of the key insights into the functions of Wnt ligands have come from studies in *Drosophila melanogaster,* which has retained seven Wnt ligand genes: *Wnt1* (*wingless* (*wg*)), *Wnt5* (*Dwnt3*), *Wnt6*, *Wnt7* (*Dwnt2*), *Wnt8* (*WntD*), *Wnt9* (*Dwnt4*) and *Wnt10* (Llimargas and Lawrence, 2001; Murat et al., 2010). In *Drosophila, wg* is crucial for many different aspects of development from segmentation to growth, patterning and differentiation of the imaginal discs (Bejsovec, 2018; Klingensmith and Nusse, 1994; Swarup and Verheyen, 2012; Wodarz and Nusse, 1998). In contrast, the other six *Drosophila* Wnt genes appear to play more restricted roles during development and the functions of some ligands, for example *Wnt6* and *Wnt10,* are still unclear or unknown respectively (Murat et al., 2010). The absence of any major or obvious phenotypic effects from mutations or overexpression for many of these Wnts could be in part explained by overlapping expression and/or their acting in combinatorial landscapes (van Amerongen and Nusse, 2009). For instance, *wg* and *Wnt7* appear to act together during development of the tracheal system in *Drosophila* (Llimargas and Lawrence, 2001). Furthermore, *wg, Wnt6, Wnt9* and *Wnt10* are found in an evolutionary conserved cluster (Nusse, 2001) that contains scattered cis-regulatory elements that are able to regulate distal and proximal genes in this cluster (Koshikawa et al., 2015) (Fig 1). These cis-regulatory elements may even be shared by these Wnt genes and could explain their overlapping expression patterns in some tissues.

Two of the genes in this cluster, *wg* and *Wnt6* are ancient paralogues (Nusse, 2001) that still encode proteins more similar to each other than to any other Wnts (Janssen et al., 2010). While *wg* is expressed from early embryogenesis onwards in *Drosophila* (reviewed in Swarup and Verheyen (2012)), *Wnt6* transcripts are first detected later in diffuse domains only in the embryonic gut and subsequently in larvae, where expression overlaps with *wg* in several imaginal discs (Doumpas et al., 2013; Janson et al., 2001; Nusse, 2001) (Fig S1). There is also evidence that *wg* and *Wnt6* are co-regulated and can have similar functions. Smith-Bolton et al. (2009) showed that both *Wnt6* and *wg* appear to be involved in early cell regeneration and damage response in imaginal discs, although the exact function of *Wnt6* in these processes remains unclear. Interestingly, an enhancer (BRV118) was identified between *wg* and *Wnt6* that promotes damage-induced activation of *wg* and *Wnt6* expression, and ablation of this enhancer decreases the expression of both Wnt genes (Harris et al., 2016). Furthermore, there is also evidence that both *wg* and *Wnt6* are involved in maxillary palp (MP) development (Doumpas et al., 2013; Lebreton et al., 2008).

MPs are important olfactory organs that develop from the eye-antennal imaginal discs (Haynie and Bryant, 1986; Jurgens, 1993) (Fig 2). The MP field is positioned ventrally to the antennal field in the anterior part of the disc (Haynie and Bryant, 1986; Held Jr, 2002) (Fig 2B). The separation of the antennal and MP fields occurs during the second instar (L2) and subsequently these two tissues differentiate during the third instar (L3) and pupal stages (Lebreton et al., 2008).

MP development requires the Hox genes *Deformed* (*Dfd*) (Merrill et al., 1987) and *proboscipedia* (*pb*) (Pultz et al., 1988) (Fig 2A). *pb* is responsible for the formation of the proximal-distal axis of the MP (Percival-Smith et al., 2017) and ectopic expression of *pb* in the eye-antennal disc leads to homeotic transformation of antennae in to MPs or legs (Benassayag et al., 2003; Cribbs et al., 1995; Held Jr, 2002; Kaufman, 1978). *Dfd* is also

expressed in the MP field (Diederich et al., 1991) and loss of *Dfd* leads to a complete loss of the MPs (Merrill et al., 1987) (Fig 2).

wg is also required for the development of the MPs as well as the antennae. In the antennal primordia, *wg* is expressed from L2 onwards, while in the MP field *wg* expression appears later in early pupae. In the MP field, *wg* activates *spineless* (*ss*), which activates *distal-less* (*dll*), regulatory steps that are essential for MP development (Fig 2A) (Emmons et al., 2007; Lebreton et al., 2008). Importantly, the temporal delay in *wg* expression in the MP field is essential for MP formation, since premature *wg* expression in the MP field during L3 triggers a MP to antennal transformation (Burgess and Duncan, 1990; Lebreton et al., 2008). This suggests regulatory elements controlling the temporal expression of *wg* are crucial for MP development but these cis-regulatory elements were not identified in these previous studies.

More recently, Doumpas et al., (2013) showed that *Wnt6* is also expressed in the MP field and flies homozygous for a deletion of the first exon of this gene had no MPs (Doumpas et al., 2013). These authors suggested that either Wnt6 interacts with Wg to specify the MPs or that previous studies had actually detected Wnt6 expression and it is this ligand rather than Wg that regulates formation of MPs (Doumpas et al., 2013).

Therefore, to investigate the role of *Wnt6* and its potential functional overlap with *wg* in the regulation of MP development further, we generated a *Wnt6* null mutant using CRISPR/Cas9. In contrast with previous reports, we found that *Wnt6* does not appear to be required for MP development, instead the 5' region of this gene may in fact contain cis-regulatory elements that are essential for the expression of *wg* in the MP field. We show that loss of *Wnt6* function, however, causes a developmental delay, suggesting it may be a general regulator of growth during *Drosophila* development perhaps in combination with *wg* in the MP primordia as well as potentially in other imaginal discs and other tissues.

Results and Discussion

Analysis and comparison of Wnt6 *mutant lines*

To further study the role of *Wnt6* during MP development, we generated a new null allele of this gene (*Wnt6*{KOmche) by using CRISPR/Cas9 to insert a construct (containing the mCherry fluorescent marker) into the coding region to produce a frameshift (Fig 1B). We confirmed the position of the insertion and its effect on the *Wnt6* reading frame by sequencing and on expression with *in situ* hybridisation. *Wnt6*{KOmche} is homozygous viable and fertile, which is consistent with the previous null allele generated for *Wnt6* by deletion of the first exon – hereafter *Wnt6*{KOd} (Doumpas et al., 2013, 2015) (Fig 1B).

We first examined the MPs of both *Wnt6*{KOmche} and *Wnt6*{KOd} as well as the control line w^{1118} (Fig 3A-C,E). In contrast to Doumpas and colleagues (2013), we did not observe a complete loss of MPs for *Wnt6*{KOd} flies, however, the MPs were extremely small and malformed when compared to those of the control line (Fig 3A,B), which is not explained by differences in body size (Fig 3F,G) (Doumpas et al., 2013). Surprisingly, however, the MPs of *Wnt6*{KOmche} flies were not significantly different from the control line and were morphologically normal (Fig 3C,E).

We also found that *Wnt6*{KOmche} males have significantly larger wings compared to the control (Fig 3F) that does not appear to be a general effect of body size as assayed by tibia length (Fig 3G). Small differences were also observed among the wings of w^{1118}, *Wnt6*{KOd} and *Wnt6*{KOmche} (Fig 3F), but these likely just reflect slight differences in their overall body size (Fig 3G).

It was previously shown that the wings of *Wnt6*{KOd} flies have perturbed spacing of the chemosensory bristles on the wing margins (Doumpas et al., 2013). We found that *Wnt6*{KOmche} flies had a very similar phenotype (Fig S2). The consistency of this phenotype between the two lines suggests it is caused by the loss of *Wnt6*.

We also noticed that both *Wnt6* mutant lines appeared to develop more slowly than the control lines. Therefore, we investigated this further by quantifying the timing to puparium formation of both *Wnt6*{KOd} and *Wnt6*{KOmche} compared to a control line (Fig S2). We observed that both *Wnt6*{KOd} and *Wnt6*{KOmche} needed significantly more time to reach pupariation compared to w^{1118} (Fig S2). This observation suggests that the loss of *Wnt6* increases the time taken for the development from larvae to pupae. Therefore, *Wnt6* could be involved in generally regulating and coordinating the growth of imaginal discs and potentially other tissues in *Drosophila*.

Our analysis of the two *Wnt6* mutant lines shows that, on the one hand, both have consistently similar defects in the spacing between chemosensory bristles and delay in developmental timing, but on the other hand only *Wnt6*{KOd} flies have small and malformed MPs. We hypothesised that this could be a consequence of the difference in the molecular lesions in these two mutants. While *Wnt6*{KOd} has a deletion of the first exon of *Wnt6*, *Wnt6*{KOmche} only has an insertion that produces a frameshift without removing any of the *Wnt6* locus (Fig 1B).

To investigate whether the deletion of the first exon of *Wnt6* may underlie the MP phenotype, we crossed the two *Wnt6* knockout lines to produce flies homozygous for loss of *Wnt6* function, but only heterozygous for the deletion of the first exon region (i.e. *Wnt6*{KOd}/*Wnt6*{KOmche}). Our results show, that *Wnt6*{KOmche}/*Wnt6*{KOd} MPs (Fig 3D) are actually significantly larger than *Wnt6*{KOmche} (and *Wnt6*{KOd}) males and females ($p < 0.001$) and control females ($p < 0.01$) (Fig 3E), which may be a consequence of a difference in overall body size as somewhat reflected by tibia differences (Fig 3G).

Taken together, our analyses of *Wnt6*{KOmche} and *Wnt6*{KOd} flies suggest that while they are both *Wnt6* null mutants, general loss of *Wnt6* function does not appear to affect the MPs, but that the deletion of the first exon of *Wnt6*, independently of *Wnt6* function, is responsible for the smaller MPs of *Wnt6*{KOd} flies.

Interaction between the Wnt6 *and* wg *loci*

In *Drosophila, wg* has also been shown to play a crucial role in MP development (Lebreton et al., 2008). This gene is the very next gene upstream of *Wnt6* and it has been suggested that they could share cis-regulatory elements (Harris et al., 2016) (Fig 1). Curiously, Doumpas *et al.* (2013) also showed that Wg expression in the MP field is lost in *Wnt6*{KOd} flies. In light of our results, we hypothesised that the lack of Wg in the MP field could be caused by the deletion in *Wnt6*{KOd} because regulatory information required for *wg* expression in developing MPs could have been removed. We therefore investigated the expression of *Wnt6* and *wg* in the developing MP field further.

To visualise the protein distribution of Wnt6, we generated an 2xHA tagged Wnt6 line using CRISPR/Cas9 (*Wnt6*{HA}). We assayed the expression of HA-Wnt6, Wg and Dfd (as a marker for the MP field) in eye imaginal discs at late L3 and pre-pupal stages (Fig 4 A-B'''). We observed overlapping expression of Wg and HA-Wnt6 in the dorsal region of the antennal field, as previously described for the mRNA expression of these genes (Doumpas et al., 2013; Janson et al., 2001) (Figs 4A, B and S1). In addition, we observed Wg expression and relatively weaker, more diffuse, HA-Wnt6 expression at late L3 in the MP field (Fig 4A-A'''). In pre-pupae, HA-Wnt6 expression was reduced in the dorsal part of the antennal field, but was still observed in the MP field. At this stage, strong expression of Wg was still detected in the dorsal antennal field and in the MP field, where its expression appeared to be more tightly localised, but stronger than HA-Wnt6 (Fig 4B-B'''). Overall, our results show that Wnt6 and Wg are expressed in overlapping patterns in the MP field.

We then compared Wg expression in the MP field between the *Wnt6*{KOd} and *Wnt6*{KOmche} lines (Fig 4C-D''). In *Wnt6*{KOmche}, strong expression of Wg could clearly be detected in the MP field that was comparable in strength to Wg expression in the antennal field (Fig 4D-D''). However, in the developing MPs of *Wnt6*{KOd} at the prepupae stage,

194 only very faint expression of Wg was observed, which was noticeably weaker than Wg
195 expression in the antennal field at this stage (Fig 4C-C''), and consistent with the smaller
196 adult MPs.

197 We also assayed the expression of *wg* and *Wnt6* transcripts in the developing MPs
198 of *Wnt6*{KOd} and *Wnt6*{KOmche} flies versus controls (Fig. S3). We detected *wg* mRNA in
199 the MP field of control and *Wnt6*{KOmche} pre-pupal discs, but we only observed *Wnt6*
200 mRNA in the former. In addition, we did not detect transcripts of either gene in the MP field
201 of *Wnt6*{KOd} flies (Fig S3). Thus, we were able to show that both *Wnt6* and *wg* are
202 expressed in the pre-pupal MP field, and while only *Wnt6* expression is lost in
203 *Wnt6*{KOmche} the deletion of the first exon in *Wnt6*{KOd} leads to a loss of *wg* as well as
204 *Wnt6* expression in this tissue.

205 Taken together with our finding that MPs appear to be unaffected by loss of *Wnt6*
206 function in *Wnt6*{KOmche}, these results suggest that the smaller MPs in *Wnt6*{KOd} might
207 be caused by a reduction in Wg expression. This could potentially be explained by the region
208 that is deleted in *Wnt6*{KOd} harbouring cis-regulatory elements that regulate Wg
209 expression in the MP field. Therefore, we next tested if the first exon of *Wnt6* has cis-
210 regulatory activity.

211 We identified two lines in the Flylight collection (Pfeiffer et al., 2008) that correspond
212 to the deleted region of *Wnt6* in *Wnt6*{KOd} (Fig 5A). The full first exon of *Wnt6* is included
213 in GMR25A04, while GMR25A05 overlaps with the 5' end of GMR25A04 and includes part
214 of the *Wnt6* 5'UTR (Fig 5A). We used these lines to drive UAS-CD8-GFP and visualised
215 expression using anti-CD8. GMR25A05 was able to drive strong expression in the MP field
216 in pre-pupal discs that overlapped with Dfd and Wg expression (Fig 4B-B'''). GMR25A04
217 was able to drive expression in a similar pattern albeit this appeared to be weaker than with
218 GMR25A05 (Fig 5C-C'''). This suggests that these regions of the *Wnt6* locus could contain
219 transcription factor binding sites that can drive expression in the MP field. Removal of the

first exon of *Wnt6,* as in the *Wnt6*{KOd} mutant line, could remove these binding sites and explain the reduction in Wg expression and the smaller MPs of this line. It has to be noted, however, that two other driver lines containing DNA directly upstream of the GMR25A05 are also able to drive expression in the MP field (Pfeiffer et al., 2008), and so, the deletion in the *Wnt6*{KOd} mutant line may also disrupt the function of these putative regulatory elements. Based on *Wnt6* expression pattern, we suggest that the *Wnt6* locus is likely to be involved in the regulation of the palps by controlling the temporal expression of Wg, but Wnt6 is not required for palp specification.

Conclusions

Our findings, together with previous studies, indicate that both *wg* and *Wnt6* are expressed in the MP field, but only the former is necessary for MP formation, since our *Wnt6* mutant still has *wg* expression in the MP field and has no effect on MP size and morphology. Thus, it appears that the first exon of *Wnt6* contain cis-regulatory elements that might regulate the expression of Wg in the MP field. These results provide new insights into the regulation and function of Wnt genes.

Enhancers that drive specific temporal and spatial *wg* expression in *Drosophila* embryos and in imaginal discs have been found upstream of this gene (e.g. Bell et al. (2019)) within its introns (e.g. Bell et al. (2019), Neumann and Cohen (1996)) in the downstream intergenic region between *wg* and *Wnt6* (Ekas et al., 2006; Harris et al., 2016; Pereira et al., 2006), downstream of *Wnt6* (Koshikawa et al., 2015) and even in the intron of the more distal *Wnt10* in the case of *D. guttifera* (Koshikawa et al., 2015). Furthermore, it has been shown that at least some of these enhancers regulate other Wnt genes (Harris et al., 2016). Our study also provides further indication that Wnt genes in the *Wnt9-wg-Wnt6-Wnt10* cluster are not only regulated by distal regulatory elements, but that these may be shared by multiple Wnt genes. This may help to explain why these Wnt genes may overlap in many

aspects of their expression (Janssen et al., 2010; Koshikawa et al., 2015; Nusse, 2001) and perhaps operate in combinatorial landscapes during development (van Amerongen and Nusse, 2009). Therefore, more systematic analysis of gene specific and shared enhancers throughout the *Wnt9-wg-Wnt6-Wnt10* region is needed to understand the cis-regulatory logic of this important gene cluster and how shared elements may have contributed to its evolutionary conservation and functionality.

Material and Methods

Fly husbandry and stocks

All fly stocks were kept at 25°C under a 12/12 dark/light cycle on standard fly food. The *Wnt6* mutant line (*Wnt6*{KOd}) was kindly provided by Aurelio Teleman (DKFZ, Germany). The following stocks were obtained from the Bloomington Drosophila Stock Centre (Indiana University, Bloomington): UAS-CD8-GFP (BDSC#32185), FlyLight lines GMR25A04 (BDSC#45137) and GMR25A05 (BDSC#45138). The *Wnt6* mutant line containing the mCherry marker insertion, referred to as Wnt6{KOmche} and a fly line containing a 2xHA tag, hereafter Wnt6{HA}, were generated in this study using CRISPR/Cas9 (see below).

Cloning and transgenesis

CRISPR/Cas9 was used to insert a 1.5 kb fragment containing the marker mCherry under the control of a *Pax* enhancer into the coding sequence of *Wnt6*. For this we used ~1 kb homology arms generated using the following primers: HA1Fwd CCTCGAATGTGTGCGTCTTG; HA1Rev CATTGCGAATATTAAAATTGCAATTACCAT; HA2Fwd ATTCGGCTGGTAAGTGGCATTTAAATAC; HA2Rev ACTTGTGTGTTAGAAGGAAGCCCC. Both homology arms were cloned into the final vector pTV3 (Baena-Lopez et al., 2013), kindly provided by Cyrille Alexandre (Francis Crick Institute, London). The guide-RNA (gRNA) sequence (GACTGGATTCGGCTGGTAAG) was chosen using the flyCRISPR website prediction tool (Gratz et al., 2014).

To generate *Wnt6*{HA}, a CRISPR/Cas9 strategy was designed to insert a 2xHA tag precisely after the *Wnt6* signal peptide, in frame with the following coding sequence using a gRNA (GCCCTCCGCCCTGAAAATAG) that cuts as close to this position as possible. Homology arms of 1 kb and 0.53 kb flanking the targeted region of the *Wnt6* gene were generated using following primers (HA1Fwd ACGTTCACACATACTTGCTCCCACCAATAT; HA1Rev CGCCCTGAAAATAGAGGAATCATAGG TTTG; HA2Fwd

GAGGGCACCAACATCCTTCT; HA2Rev GGCTCATTTCAGGCGCTATT). The homology arms were cloned into the vector $IO_{2xHA@N}$TV-Pax-Cherry (kindly provided by Cyrille Alexandre, Francis Crick Institute, London). Both homology arms were inserted into the vector using the SLIC method (Li and Elledge, 2012). Plasmids were injected by BestGene (Chino Hills, USA) into a *D. melanogaster* stock containing an endogenous *nanos-Cas9* on the third chromosome (CAS-0003).

Gene expression analysis

Eye-antennal imaginal discs were dissected from wandering third instar larvae (L3) and pre-pupal (white pupae) and fixed in 4% formaldehyde in PBS + 0.2% Triton 100. For antibody stainings, the following primary antibodies were used: anti-HA monoclonal rabbit antibody (1:100) (Sigma Aldrich #H6908), anti-Wg 4D4 monoclonal mouse antibody (DSHB) (1:100), anti-Deformed monoclonal guinea pig (1:250) (kind gift from Ingrid Lohmann, University of Heidelberg) and anti-CD8 monoclonal rabbit (1:500) antibody (Abcam #ab101500). The secondary antibodies, Alexa Fluor 647 anti-mouse, 488 anti-rabbit and 594 anti-guinea pig (all Invitrogen) were used at 1:1000. All tissues were additionally stained with Hoechst dye, mounted on Poly-L-Lysin coated coverslips and embedded in 100% glycerol. Images were taken using a Leica Sp8 confocal microscope and analysed using Fiji 2.0.0-rc-65/1.52b (Schindelin et al., 2012).

For *in situ* hybridisation, L3 and pre-pupal eye-antennal imaginal discs were dissected in 1 x PBS on ice and fixed for 20 minutes in 4% formaldehyde in PBS-T (1x PBS + 0.2% Tween 20). Tissues were treated with Proteinase K (1:2000), re-fixed and hybridised at 56°C overnight with the probe (*wg* or *Wnt6*) in hybridisation buffer (50% formamide, 5x SSC pH 7.0, 10 mg/ml salmon sperm, 1 mg/ml tRNA, 100 µg/ml heparin and 0.2% Tween 20, adjust pH 6.5 with 1M HCl). After hybridisation, tissues were blocked with 1x blocking reagent (Roche) and incubated with the Anti-Fab AP Fragment antibody (Roche, 1:2000) in 1x

blocking reagent (Roche). All discs were stained with NBT/BCIP (Roche) in the AP staining buffer (100 mM NaCl, 50 mM MgCl2, 100 mM Tris HCl pH 9.5 and 0.2% Tween 20). Staining was stopped by several washes with PBS-T. Note that reactions with the same probe were always stopped at the same time (after up to 45 mins), but sometimes staining was extended for an extra 20 mins to verify expression was missing in the MP field of some samples relative to controls that showed expression in this region. Discs were then mounted on Poly-L-Lysine slides in 100% glycerol and imaged using a Zeiss AxioZoom.V16 microscope with an Axiocam 506 colour camera or a Zeiss Cell Observer.Z1 with a Axiocam MRc colour camera.

Phenotypic analysis

Three days after eclosion, female and male flies were collected and stored in 70% ethanol. The second pair of legs and the wings were dissected and mounted in Euparal (ALS Hindolveston, Norfolk). MPs were dissected in 70% ethanol and mounted in Hoyer's medium on slides, heated overnight at 60°C. Measurements of the second leg tibia was used as a proxy for body size (Fig 3). For wing bristles measurements, the spacing between 10 chemosensory bristles per wing (n = 30) of lines w^{1118}, *Wnt6*{KOd} and *Wnt6*{KOmche} were counted using the number of mechanosensory bristles (after Doumpas et al. 2013). MPs and the wings for the bristle analysis were imaged using a Zeiss Axioplan microscope, all other wings and legs were imaged using a Zeiss Axiozoom microscope. All dissections were measured using ImageJ 1.48v (Schneider et al., 2012).

To analyse the developmental time from egg to pupa of *Wnt6* mutant and control lines, 30 eggs were collected from 1 to 2 hours egg lays and placed into a fly food vial in three replicates for each line. The vials were monitored throughout the following 145 hours twice a day and from 4th day after egg lay (wandering larvae) every hour until all wandering larvae pupariated. For each line, the number of pupae in three replicate vials were counted.

331

332 *Statistical analysis*

333 All data was analysed using RStudio version 1.1.463 (R_Core_Team, 2018). Differences
334 between MP areas, wing and leg lengths were tested using a one-way ANOVA followed by
335 a Tukey's HSD test. In all analyses, female and male measurements were assessed
336 separately. All data was tested for normality using a Shapiro-Wilks test.

Acknowledgements

We would like to thank Alberto Baena-Lopez (University of Oxford), JP Vincent and Cyrille Alexandre (Francis Crick Institute, London) for discussion and contribution of materials. The authors also thank Javier Figueras Jimenez for his help with larval dissections and fixation. We thank Michael Boutros for the support of MH to complete the project and Aurelio Teleman for discussion of the results. MH was funded by Nigel Groome PhD studentship from Oxford Brookes University and during manuscript preparation and revisions by the Deutsche Forschungsgemeinschaft (DFG, German Research Foundation) – Projektnummer 331351713 – SFB 1324 (project A01 to Michael Boutros). FAF was funded by a DFG Research Fellowship (FR 3929/1-1).

References

Baena-Lopez, L.A., Alexandre, C., Mitchell, A., Pasakarnis, L., Vincent, J.P., 2013. Accelerated homologous recombination and subsequent genome modification in Drosophila. Development 140, 4818-4825.

Bejsovec, A., 2018. Wingless Signaling: A Genetic Journey from Morphogenesis to Metastasis. Genetics 208, 1311-1336.

Bell, K., Skier, K., Chen, K.H., Gergen, J.P., 2019. Two pair-rule responsive enhancers regulate wingless transcription in the Drosophila blastoderm embryo. Dev Dyn.

Benassayag, C., Plaza, S., Callaerts, P., Clements, J., Romeo, Y., Gehring, W.J., Cribbs, D.L., 2003. Evidence for a direct functional antagonism of the selector genes *proboscipedia* and *eyeless* in *Drosophila* head development. Development 130, 575.

Burgess, E.A., Duncan, I., 1990. Direct control of antennal identity by the spineless-aristapedia gene of Drosophila. Molecular and General Genetics MGG 221, 347-352.

Cho, S.J., Valles, Y., Giani, V.C., Jr., Seaver, E.C., Weisblat, D.A., 2010. Evolutionary dynamics of the wnt gene family: a lophotrochozoan perspective. Mol Biol Evol 27, 1645-1658.

Cribbs, D.L., Benassayag, C., Randazzo, F.M., Kaufman, T.C., 1995. Levels of homeotic protein function can determine developmental identity: evidence from low-level expression of the Drosophila homeotic gene proboscipedia under Hsp70 control. The EMBO journal 14, 767-778.

Diederich, R.J., Pattatucci, A.M., Kaufman, T.C., 1991. Developmental and evolutionary implications of labial, Deformed and engrailed expression in the Drosophila head. Development 113, 273.

Doumpas, N., Jekely, G., Teleman, A.A., 2013. Wnt6 is required for maxillary palp formation in Drosophila. BMC Biol 11, 104.

374 Doumpas, N., Jekely, G., Teleman, A.A., 2015. Erratum to: Wnt6 is required for maxillary
375 palp formation in Drosophila. BMC Biol 13, 100.
376 Ekas, L.A., Baeg, G.-H., Flaherty, M.S., Ayala-Camargo, A., Bach, E.A., 2006. JAK/STAT
377 signaling promotes regional specification by negatively regulating
378 wingless expression in <em>Drosophila</em&gt. Development
379 133, 4721.
380 Emmons, R.B., Duncan, D., Duncan, I., 2007. Regulation of the Drosophila distal antennal
381 determinant spineless. Developmental Biology 302, 412-426.
382 Gratz, S.J., Ukken, F.P., Rubinstein, C.D., Thiede, G., Donohue, L.K., Cummings, A.M.,
383 O'Connor-Giles, K.M., 2014. Highly specific and efficient CRISPR/Cas9-catalyzed
384 homology-directed repair in Drosophila. Genetics 196, 961-971.
385 Harris, R.E., Setiawan, L., Saul, J., Hariharan, I.K., 2016. Localized epigenetic silencing of
386 a damage-activated WNT enhancer limits regeneration in mature Drosophila imaginal discs.
387 Elife 5.
388 Haynie, J.L., Bryant, P.J., 1986. Development of the eye-antenna imaginal disc and
389 morphogenesis of the adult head in Drosophila melanogaster. J Exp Zool 237, 293-308.
390 Held Jr, L.I., 2002. Imaginal Discs: The Genetic and Cellular Logic of Pattern Formation.
391 Cambridge University Press, Cambridge.
392 Janson, K., Cohen, E.D., Wilder, E.L., 2001. Expression of DWnt6, DWnt10, and DFz4
393 during Drosophila development. Mechanisms of Development 103, 117-120.
394 Janssen, R., Le Gouar, M., Pechmann, M., Poulin, F., Bolognesi, R., Schwager, E.E.,
395 Hopfen, C., Colbourne, J.K., Budd, G.E., Brown, S.J., Prpic, N.M., Kosiol, C., Vervoort, M.,
396 Damen, W.G., Balavoine, G., McGregor, A.P., 2010. Conservation, loss, and redeployment
397 of Wnt ligands in protostomes: implications for understanding the evolution of segment
398 formation. BMC Evol Biol 10, 374.
399 Jurgens, G., Hartenstein, V. , 1993. The development of Drosophila melanogaster.

Kaufman, T.C., 1978. Cytogenetic Analysis of Chromosome 3 in DROSOPHILA MELANOGASTER: Isolation and Characterization of Four New Alleles of the Proboscipedia (pb) Locus. Genetics 90, 579-596.

Klingensmith, J., Nusse, R., 1994. Signaling by wingless in Drosophila. Developmental Biology 166, 396-414.

Koshikawa, S., Giorgianni, M.W., Vaccaro, K., Kassner, V.A., Yoder, J.H., Werner, T., Carroll, S.B., 2015. Gain of cis-regulatory activities underlies novel domains of wingless gene expression in Drosophila. Proceedings of the National Academy of Sciences 112, 7524.

Lebreton, G., Faucher, C., Cribbs, D.L., Benassayag, C., 2008. Timing of Wingless signalling distinguishes maxillary and antennal identities in Drosophila melanogaster. Development 135, 2301-2309.

Lengfeld, T., Watanabe, H., Simakov, O., Lindgens, D., Gee, L., Law, L., Schmidt, H.A., Ozbek, S., Bode, H., Holstein, T.W., 2009. Multiple Wnts are involved in Hydra organizer formation and regeneration. Dev Biol 330, 186-199.

Li, M.Z., Elledge, S.J., 2012. SLIC: a method for sequence- and ligation-independent cloning. Methods Mol Biol 852, 51-59.

Llimargas, M., Lawrence, P.A., 2001. Seven Wnt homologues in Drosophila: a case study of the developing tracheae. Proc Natl Acad Sci U S A 98, 14487-14492.

Logan, C.Y., Nusse, R., 2004. The Wnt signaling pathway in development and disease. Annu Rev Cell Dev Biol 20, 781-810.

Merrill, V.K., Turner, F.R., Kaufman, T.C., 1987. A genetic and developmental analysis of mutations in the Deformed locus in Drosophila melanogaster. Developmental biology 122, 379-395.

Murat, S., Hopfen, C., McGregor, A.P., 2010. The function and evolution of Wnt genes in arthropods. Arthropod Struct Dev 39, 446-452.

Neumann, C.J., Cohen, S.M., 1996. Distinct mitogenic and cell fate specification functions of wingless in different regions of the wing. Development 122, 1781-1789.

Nusse, R., 2001. An ancient cluster of Wnt paralogues. Trends in genetics : TIG 17, 443.

Percival-Smith, A., Ponce, G., Pelling, J.J., 2017. The Noncell Autonomous Requirement of Proboscipedia for Growth and Differentiation of the Distal Maxillary Palp during Metamorphosis of Drosophila melanogaster. Genet Res Int 2017, 2624170.

Pereira, P.S., Pinho, S., Johnson, K., Couso, J.P., Casares, F., 2006. A 3′ cis-regulatory region controls wingless expression in the Drosophila eye and leg primordia. Developmental Dynamics 235, 225-234.

Pfeiffer, B.D., Jenett, A., Hammonds, A.S., Ngo, T.-T.B., Misra, S., Murphy, C., Scully, A., Carlson, J.W., Wan, K.H., Laverty, T.R., Mungall, C., Svirskas, R., Kadonaga, J.T., Doe, C.Q., Eisen, M.B., Celniker, S.E., Rubin, G.M., 2008. Tools for neuroanatomy and neurogenetics in Drosophila. Proceedings of the National Academy of Sciences 105, 9715.

Prud'homme, B., Lartillot, N., Balavoine, G., Adoutte, A., Vervoort, M., 2002. Phylogenetic Analysis of the Wnt Gene Family: Insights from Lophotrochozoan Members. Current Biology 12, 1395-1400.

Pultz, M.A., Diederich, R.J., Cribbs, D.L., Kaufman, T.C., 1988. The proboscipedia locus of the Antennapedia complex: a molecular and genetic analysis. Genes & development 2, 901-920.

R_Core_Team, 2018. R: A language and environment for statistical computing. R Foundation for Statistical Computing, Vienna, Austria. .

Schindelin, J., Arganda-Carreras, I., Frise, E., Kaynig, V., Longair, M., Pietzsch, T., Preibisch, S., Rueden, C., Saalfeld, S., Schmid, B., Tinevez, J.Y., White, D.J., Hartenstein, V., Eliceiri, K., Tomancak, P., Cardona, A., 2012. Fiji: an open-source platform for biological-image analysis. Nat Methods 9, 676-682.

Schneider, C.A., Rasband, W.S., Eliceiri, K.W., 2012. NIH Image to ImageJ: 25 years of image analysis. Nature Methods 9, 671.

Smith-Bolton, R.K., Worley, M.I., Kanda, H., Hariharan, I.K., 2009. Regenerative growth in Drosophila imaginal discs is regulated by Wingless and Myc. Dev Cell 16, 797-809.

Swarup, S., Verheyen, E.M., 2012. Wnt/Wingless signaling in Drosophila. Cold Spring Harb Perspect Biol 4.

van Amerongen, R., Nusse, R., 2009. Towards an integrated view of Wnt signaling in development. Development 136, 3205-3214.

Wiese, K.E., Nusse, R., van Amerongen, R., 2018. Wnt signalling: conquering complexity. Development 145.

Wodarz, A., Nusse, R., 1998. MECHANISMS OF WNT SIGNALING IN DEVELOPMENT. Annual Review of Cell and Developmental Biology 14, 59-88.

Figure legends

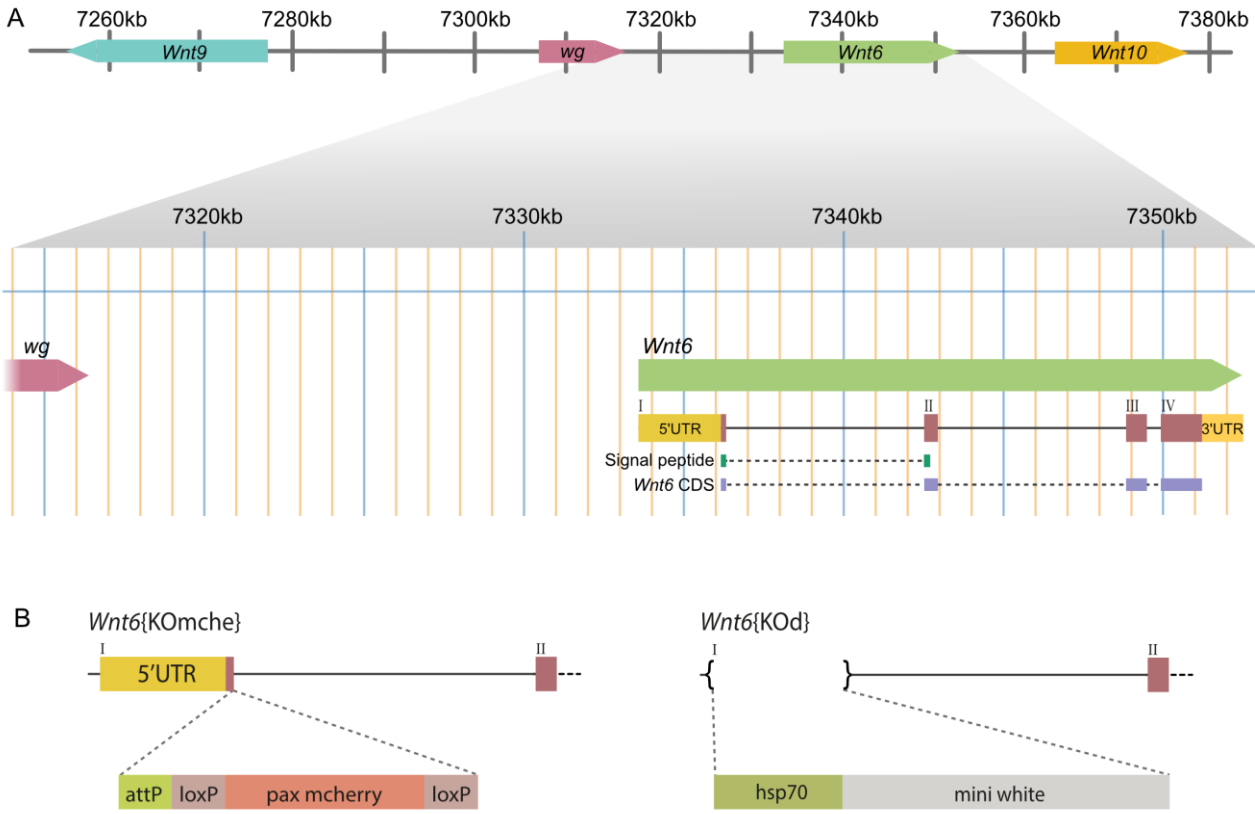

Fig 1. The genomic location of *wg* and *Wnt6*.

(A) *Wnt6* and *wg* are located 17 kb apart on the chromosome arm 2L in *Drosophila,* forming the middle of the *Wnt9-wg-Wnt6-Wnt10* cluster. *Wnt6* contains four exons (I-IV) with the first and second exon encoding the signal peptide sequence. The first exon mainly contains the 5'UTR. **(B)** Schematic drawing of the two *Wnt6* mutant lines used in this study. *Wnt6*{KOmche} was created using CRISPR/Cas9 to insert a marker into the first exon, interrupting the signal peptide and reading frame of *Wnt6*. The *Wnt6*{KOd} line was created by Doumpas *et al.,* (2013) by deletion and replacement of the whole first exon of *Wnt6*.

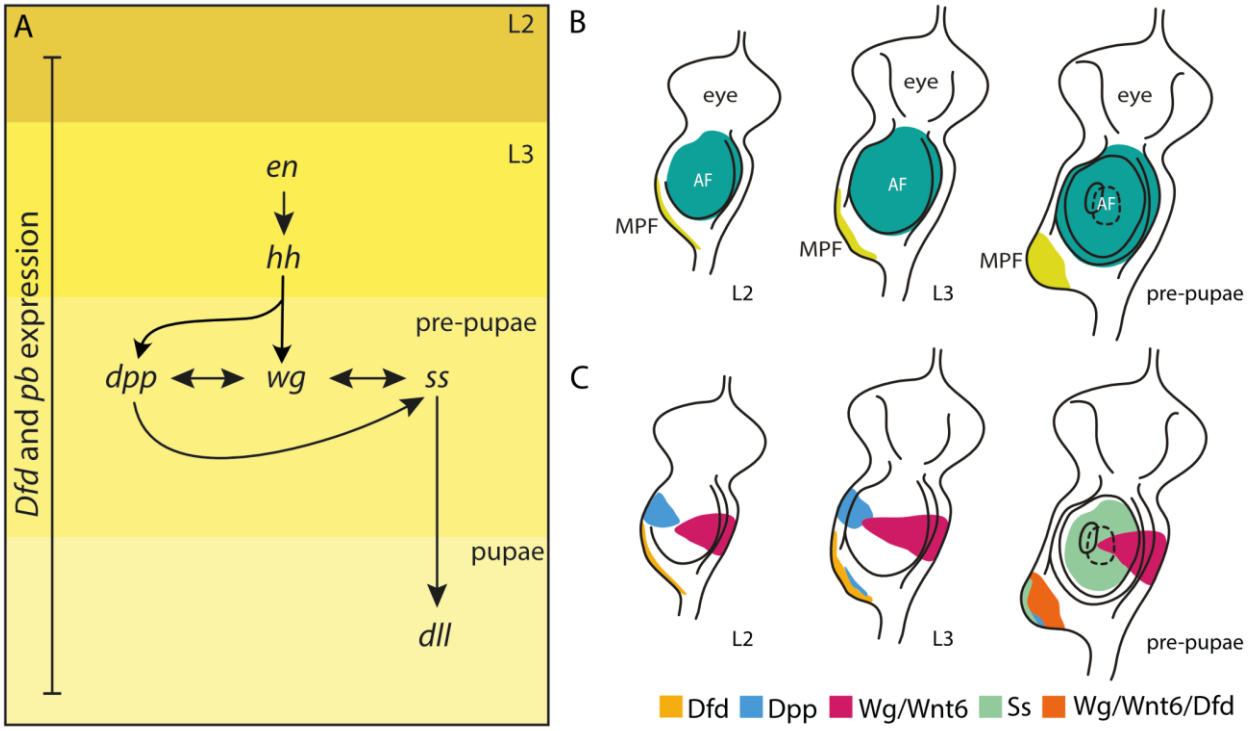

Fig 2. Maxillary palp development in *Drosophila melanogaster*.

(A) Summary of the regulation of maxillary palp (MP) development based on Lebreton *et al.*, (2008). MP determination occurs during L2, when expression of *Dfd* and *pb* first appears. During L3, *en* activates *hh,* which activates *wg* and *dpp* in pre-pupae. *wg* and *dpp* both then initiate expression of *ss* in pre-pupae. *ss* then activates *Dll* expression in the MP field. **(B)** Schematic drawing of a developing eye imaginal disc highlighting three mophological domains: the antennal field (AF), maxillary palp field (MPF) and eye primordia. **(C)** Overview of the spatial expression patterns of key genes in MP development. All disc schematics are oriented with anterior to the left.

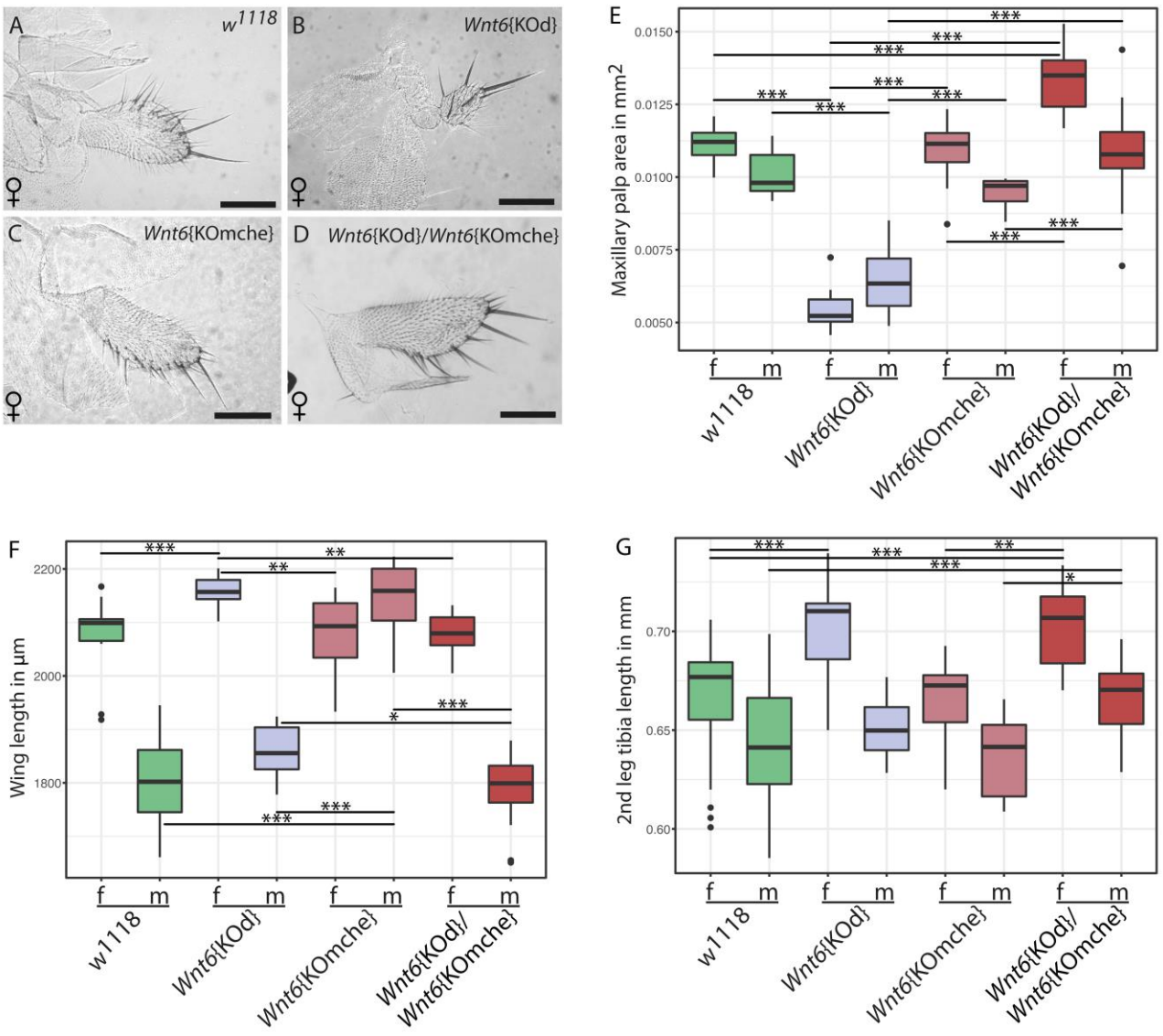

Fig 3. Maxillary palps, wings and tibias of control and *Wnt6* mutants

(A) Maxillary palps of females from w^{1118}, **(B)** *Wnt6*{KOd}, **(C)** *Wnt6*{KOmche} and **(D)** *Wnt6*{KOd}/*Wnt6*{KOmche}. **(E)** Analysis of the MP area of all lines used. **(F)** Wing length measurements and **(G)** the length of the 2nd leg tibia as proxies for body size. Significant differences were tested using a one-way ANOVA (df=7; $F\text{-value}_{MP}$=106.1; $F\text{-value}_{Wing}$=108.8; $F\text{-value}_{Leg}$=20.73) followed by a Tukey HSD test. * p<0.05; ** p<0.01; *** p<0.001; f: female; m: male.

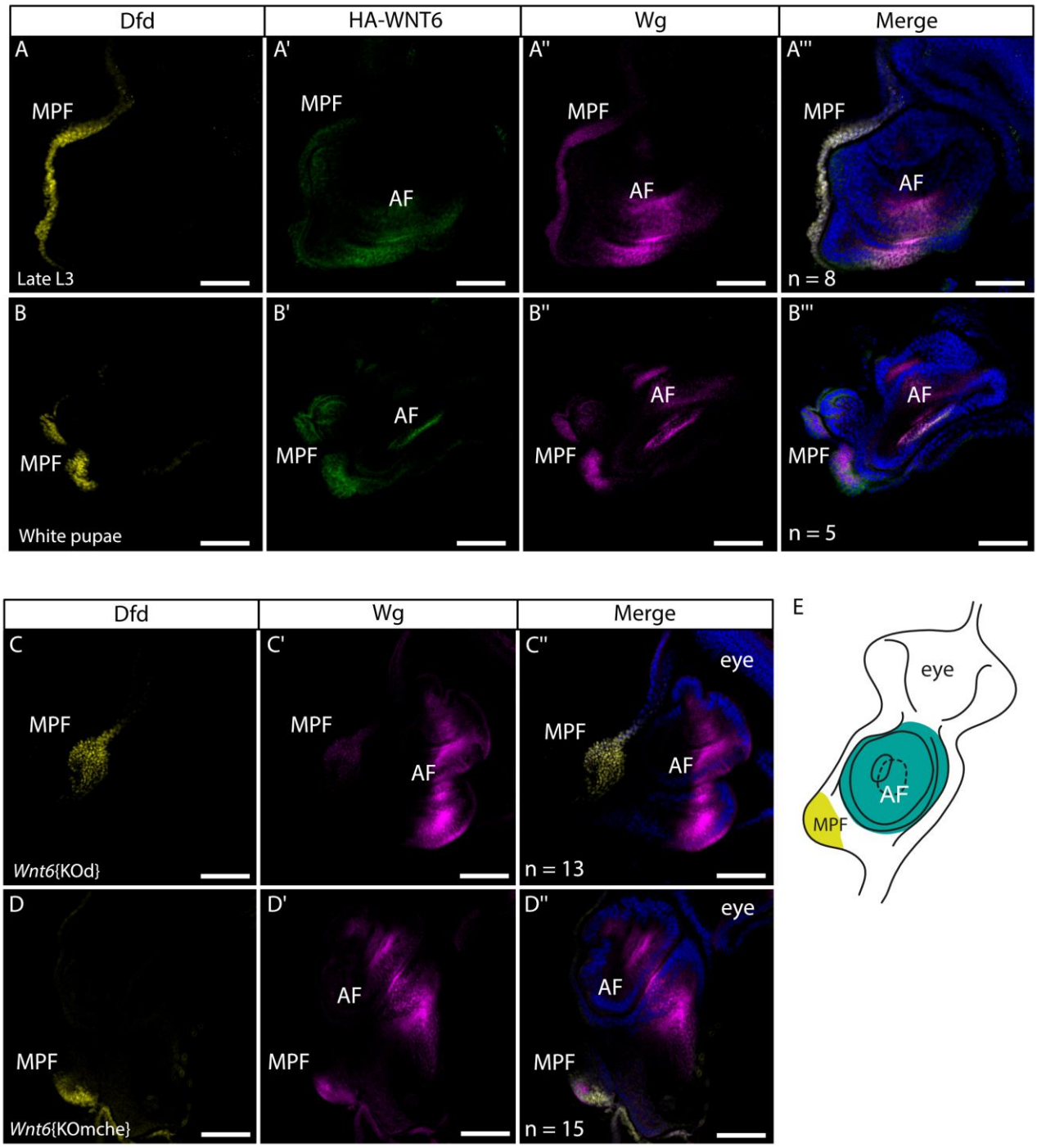

Fig 4. Wnt6 and Wg expression in eye-antennal imaginal discs

(A-A’’’) Expression of HA-Wnt6 in eye-antennal discs of late L3 and **(B-B’’’)** pre-pupal stages. (**A** and **B**) Expression of anti-Dfd, indicating the developing MP field. (**A’** and **B’**) Expression of anti-HA-Wnt6, indicating similar expression domains of Wnt6 and Wg. (**A’’** and **B’’**) Wg expression can be seen in the AF and MP field at both stages. (**A’’’** and **B’’’**) Merge of all channels shows the strong colocalization of Dfd, Wnt6 and Wg in the MP field

in L3 and pre-pupal stages. **(C-D'')** Expression of Dfd and Wg in the Wnt6 mutant lines in pre-pupal eye discs. (**C**-**C''**) anti-Dfd (**C**) and anti-Wg (**C'**) in the *Wnt6{KOd}* line. Weak expression of Wg can be detected in the MP field. (**D**-**D''**) anti-Dfd (**D**) and anti-Wg (**D'**) expression in *Wnt6{KOmche}* indicating strong Wg expression in the MP field. **(E)** Schematic drawing of the eye disc orientation in the presented pictures in **A** to **D'''**. All discs are orientated with anterior to the top and ventral to the left. MPF: maxillary palp field; AF: antennal field. Sample sizes are indicated for each strain in the merged image. Scale bar: 200 µm.

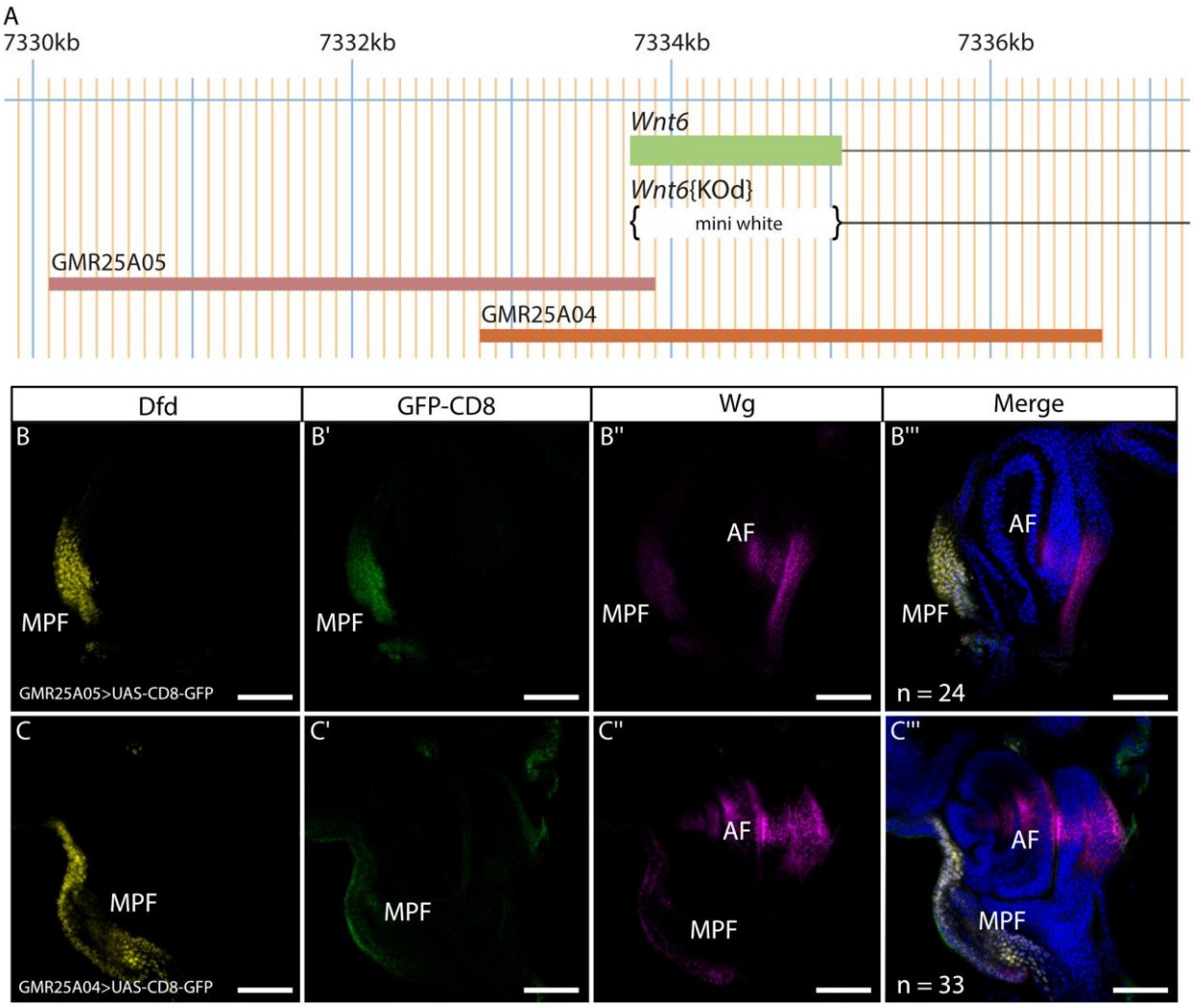

Fig 5. Assaying the activity of the putative regulatory region in pre-pupal eye imaginal discs.

(A) Schematic overview of the genomic location present in the two used FlyLight lines, GMR25A04 and GMR25A05, the *Wnt6* locus and the deletion of the *Wnt6*{KOd} line. **(B-B'')** Expression of anti-Dfd (**B**) indicates the MP field in flies from the GMR25A05>UAS-CD8-GFP cross, while expression of anti-CD8 (**B'**) can be seen in the MP field as well as Wg (**B''**). Expression of GFP indicates regulatory activity of GMR25A05 in the MP field. **(C-C'')** In GMR25A04>UAS-CD8-GFP, weaker expression of anti-CD8 (**C'**) can be detected in the MPF, marked by anti-Dfd (**C**) while similar anti-Wg signal can be seen compared to

GMR25A05 line (**C’’**). MPF: maxillary palp field; AF: antennal field. Sample sizes are indicated in the merged image for each cross. Scale bar = 200 µm.

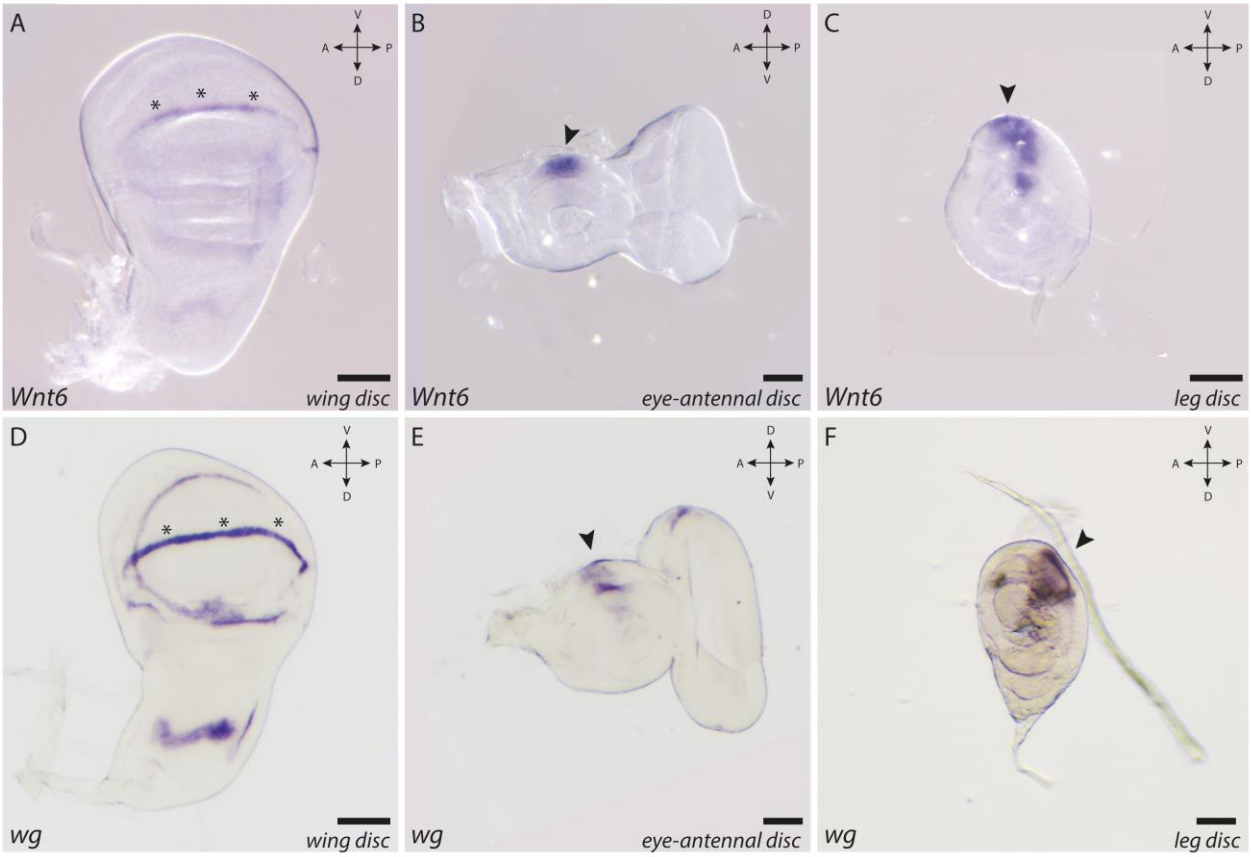

Fig S1. Overlapping expression of *Wnt6* and *wg* mRNA in imaginal discs of *Drosophila* larvae.

Expression patterns of *Wnt6* and *wg* in wandering L3 imaginal discs of w^{1118}. **(A)** *Wnt6* expression in the wing disc, **(B)** eye-antennal disc and **(C)** leg disc. **(D)** *wg* expression in the wing disc, **(E)** eye-antennal disc and **(F)** leg disc. At the dorsal-ventral border in the wing disc overlapping expression of *Wnt6* and *wg* (asterisks) can be detected. In eye-antennal and leg discs the expression of *Wnt6* and *wg* also overlap (arrowheads). Orientation of discs is indicated at right top corner. Scale bar = 200 μm.

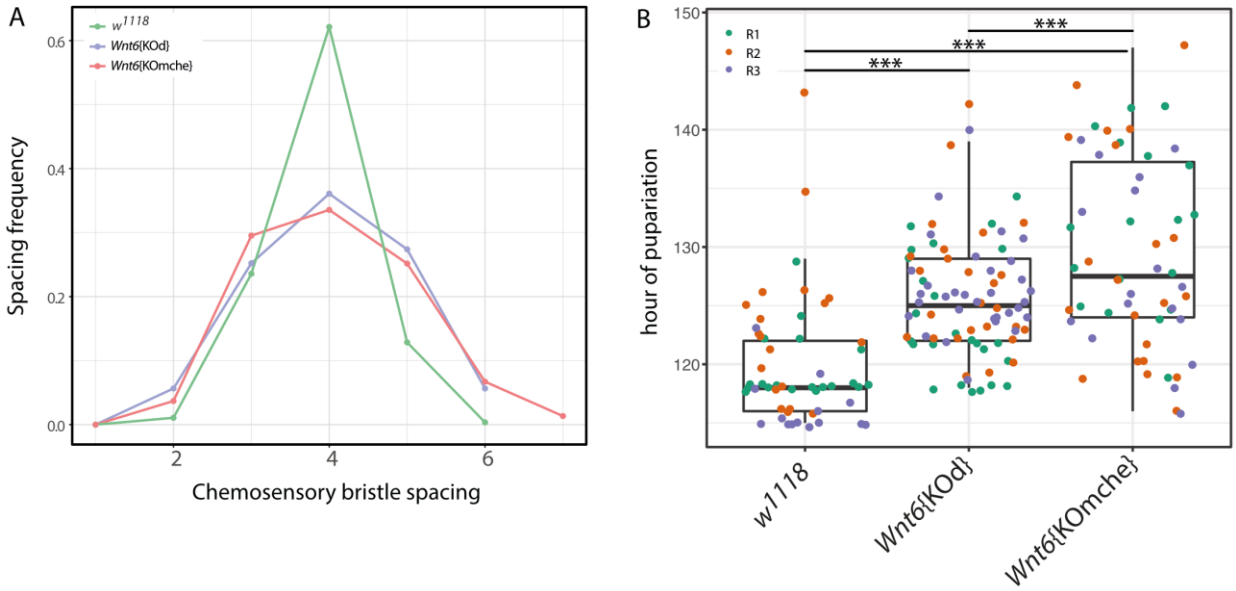

535

536 **Fig S2. Phenotypic analysis of Wnt6 mutant lines.**

537 **(A)** Analysis of the distance between chemosensory bristles using the number of
538 mechanosensory bristles along the anterior wing margin of wildtype (w^{1118}, green),
539 *Wnt6*{KOd} (light blue) and *Wnt6*{KOmche} (red). The control shows a regular spacing
540 pattern with the frequency of 0.6 between chemosensory bristles, while both *Wnt6* knockout
541 lines have greater variation in mechanosensory bristle spacing. **(B)** Time to pupariation in a
542 control line and the *Wnt6* knockout lines. Shown are three biological replicates for each of
543 the lines (R1-R3). None of the replicates for any line are significantly different from each
544 other. Both *Wnt6* mutant lines pupariate significantly later then the control line ($p<0.001$).
545 Significance was tested by one-way ANOVA (df=2; F-value=33.13) followed by a Tukey
546 HSD test. *** $p<0.001$.

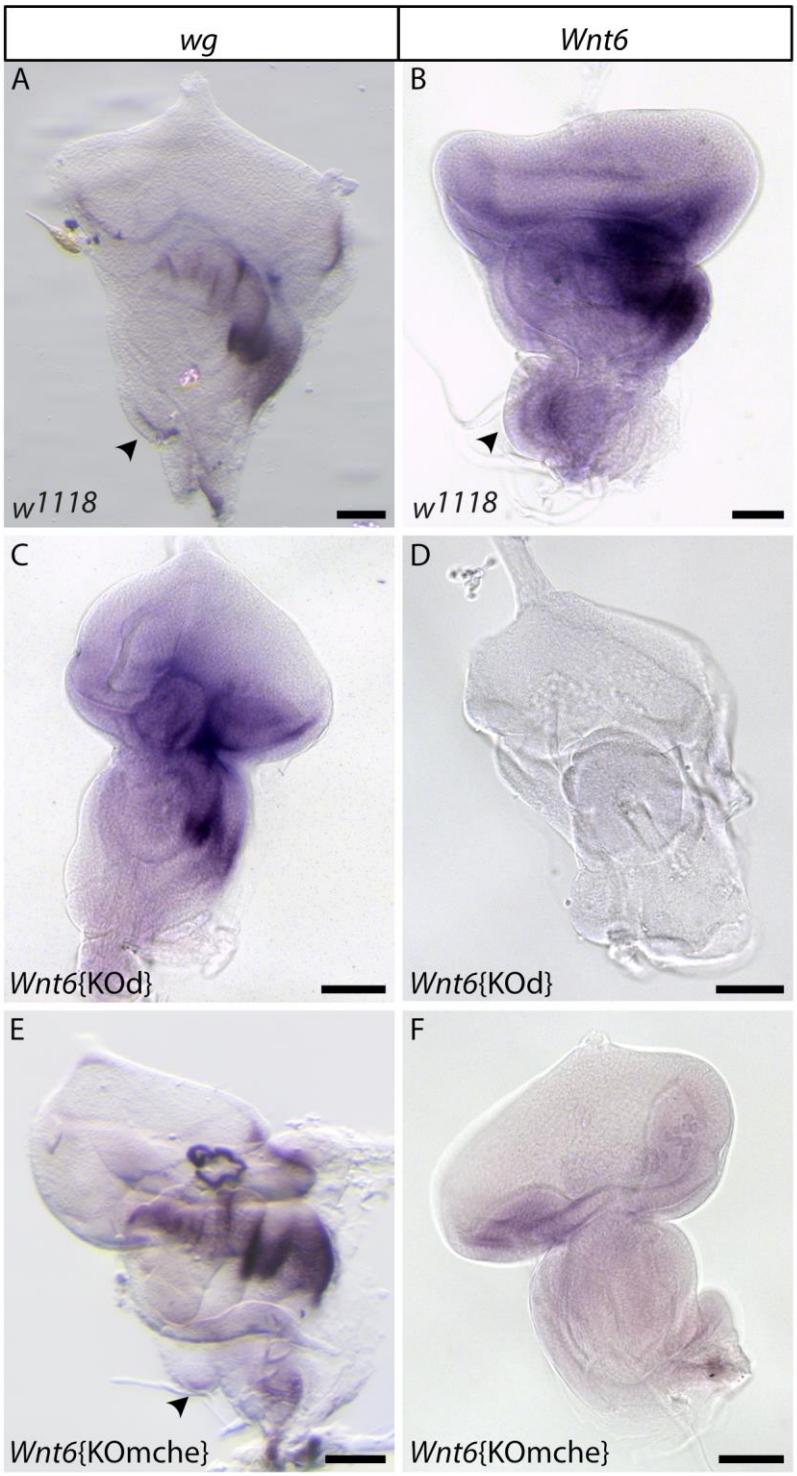

Fig S3. Expression of *wg* and *Wnt6* expression in pre-pupal eye-antennal discs.

Expression of *wg* in pre-pupal discs of the control w^{1118}, and the *Wnt6* mutants *Wnt6*{KOd} and *Wnt6*{KOmche} is shown in the left column. In the right column *Wnt6* expression is shown for the same lines. **(A and B)** The control shows *wg* and *Wnt6* expression in the MP field (arrow head), while no expression of *wg* or *Wnt6* is seen in the MP field of *Wnt6*{KOd}

553 **(C and D). (E and F)** Expression of *wg* can be detected in the MP field of *Wnt6*{KOmche}
554 while expression of *Wnt6* is absent. Anterior is positioned to the left. Scale bar = 50 μm.
555